

# Liquefaction Potential Study Due to Strong Earthquake on Reclamation Land in Northern Jakarta

M.N. Fikri<sup>1</sup>, T.F. Fathani<sup>1\*</sup>, A. Rifa'i<sup>1</sup>, L.Z. Mase<sup>2</sup>

<sup>1</sup>Departement of Civil and Environmental Engineering, Universitas Gadjah Mada, Yogyakarta, INDONESIA

<sup>2</sup>Departement of Civil Engineering, Universitas Bengkulu, Bengkulu, INDONESIA

\*Corresponding author: tfathani@ugm.ac.id

## ABSTRACT

Determining geotechnical parameters for a site is a crucial step in geotechnical analyses and designs, especially in regions prone to seismic activity, namely Liquefaction Potential Index. This study aims to evaluate the liquefaction potential in a 63-hectare reclamation land in Northern Jakarta. Both a simplified method and a multiple-segment trapezoidal method are used to identify safety factors and potential liquefaction. The analysis utilizes the Standard Penetration Test and borehole data to establish soil property indices in the research area. The likelihood of liquefaction occurrence is assessed and mapped using linear distance weighting interpolation methods, along with historical earthquake data with a magnitude of  $M_w$  7.5. The differences in the depth and thickness of sand layers in the research area lead to varying possibilities of liquefaction occurrences. The mapping results indicate no potential, marginal potential, and moderate potential are 53.26%, 37.42%, and 9.32% within the research site.

**Keywords:** Liquefaction Potential Index, Peak Ground Acceleration, Simplified Procedure, Microzonation Map.

## 1 INTRODUCTION

Jakarta is situated on the northern coast of West Java, approximately 250 km away from the Java subduction zone. However, in the last decade, residents of Jakarta experienced intense ground shaking from two events: a 7.5  $M_w$  earthquake on August 9, 2007, near Karawang, and a 7.3  $M_w$  earthquake on September 2, 2009, near Garut. The Karawang event was an intraslab earthquake at a depth of 280 km, while the Tasikmalaya event was an intra-plate earthquake at a depth of 30 km, with epicenters located 50 km and 180 km away from Jakarta, respectively (Irsyam et al., 2015). Although no damage was reported from these events, the location of the subduction could induce the potential for larger and/or closer earthquakes to pose a threat to the densely populated city of Jakarta.

In the present era, seismic phenomena are frequently associated with liquefaction events. The liquefaction incident in Palu in 2018 showcased the highly impactful consequences that can arise from liquefaction events. Generally, liquefaction phenomena lead to a sudden decrease in soil strength properties and potentially cause extensive damage to the built environment (Jalil *et al.*, 2020). Research related to liquefaction has seen significant development. Mase *et al.* (2020) conducted a study addressing the potential occurrence of liquefaction in Northern Thailand, employing methodologies involving ambient noise calculations and surface wave spectrum analysis. Additionally, another research effort led by Mase (2018) delved into the analysis of liquefaction potential through a one-dimensional non-linear site response framework. In general, the main concern of the study conducted by Mase (2018) and Jalil *et al.* (2020) focused on the coastal areas city of Bengkulu and Banda Aceh, respectively. Other extensive liquefaction studies in the Jakarta region have also been conducted, indicating a low liquefaction potential in the central areas of the province, with a tendency for increasing susceptibility observed along the northern coastal regions (Agung *et al.*, 2023; Dinata *et al.*, 2018). The research above showed that Investigations regarding the seismic and liquefaction potential in the reclamation area north of Jakarta remain relatively uncommon.

This research provides analysis and produces a microzonation map of the liquefaction potential assessment focusing on a reclamation island by using SPT data. The study commenced by initially processing soil data, including soil property indices and mechanical properties, which were employed for the computation of liquefaction potential using the simplified method proposed by Boulanger and Idriss (2014). A minimum of 16 Standard Penetration Test (SPT) and borehole locations are incorporated into the study. Geographic Information System (GIS) software, specifically Quantum Geographic Information System (QGIS), facilitates the mapping of liquefaction potential. The research concludes with the production of a spatial representation, delineating high-risk liquefaction areas within the intended development region of the reclamation island as the research area along the North Coast of Jakarta that might occur in the future.

2 MATERIAL AND METHODS

2.1 Seismotectonic settings surrounding Jakarta

Western Indonesia, where Jakarta is located, tectonically consists of the Sunda Shelf which includes the islands of Sumatra, Java, Bali, Borneo, and the southwestern part of Sulawesi (Hamilton, 1979). The active tectonics of western Indonesia is dominated by the convergence of the Australia plate with Sumatera and Java (Bock *et al.*, 2003). Seismotectonic map showing the fault locations, geological setting, and historical earthquakes surrounding Jakarta (Fig.1). Table 1 summarizes the activity both for the fault and subduction zone influencing Jakarta City in order to estimate ground shaking for scenario earthquakes in liquefaction potential. Both Figure 1 and Table 1 show that Jakarta has some earthquake potential due to its seismotectonic settings.

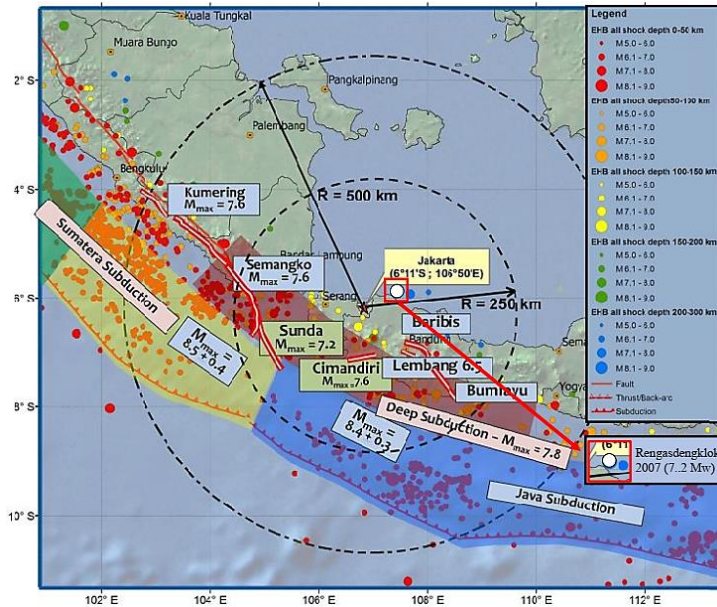


Figure 1. Seismotectonic map influencing Jakarta (modified from Irsyam *et al.*, 2015).

Table 1. Active seismic sources within a 250 km radius from Jakarta (modified from Irsyam *et al.*, 2015).

Sources	Name	Mechanism	M <sub>max</sub>	Slip Rate (mm/yr)
Fault	Cimandiri	Strike-slip	7.2	4
	Lembang	Strike-slip	6.6	1.5
	Semongko	Strike-slip	7.2	5
	Sunda	Strike-slip	7.6	5
	Kuning	Strike-slip	7.6	11.0
Subduction	South Sumatera Megathrust	Reverse	9.0	--
	Java Megathrust	Reverse	9.0	--

Table 2 presents earthquake occurrences in the Jakarta and surrounding areas. These seismic events are categorized within at least a 100 km radius with a magnitude exceeding 5 M<sub>w</sub>. and less than 300 km focal depth. Those categories are used as justification for most occurrences of earthquakes that produce fatal damage. The earthquake magnitudes are then employed for evaluating the vulnerability of the Jakarta region, particularly within the research area (reclamation land), concerning the potential for liquefaction occurrences.

Table 2. Earthquake data in Jakarta and surrounding areas.

No.	Location/Time	Coordinate		Depth (m)	Magnitude (M <sub>w</sub> )	Source
		Lat (°)	Long (°)			
1	Banten 2018	-7.21	105.91	10	6.4	BMKG
2	Jawa Barat 2009	-8.24	107.32	30	7.3	
3	Jawa Barat 2007	-6.13	107.68	284	6.9	
1	Rengasdengklok 2007	5.86	107.42	280	7.5	USGS
2	Cibinong 1974	6.51	106.83	131	6.0	
3	Pamanukan 2010	5.92	107.68	291.2	6.1	

Peak Ground Acceleration (PGA), defined as the amplitude of the largest recorded peak acceleration, is widely used to characterize the ground motion. This parameter is essential for the calculation of cyclic soil motion, represented by the maximum horizontal acceleration at the surface, widely known as  $a_{max}$ . In Jakarta itself, the PGA values range from 0.25 to 0.30 (Fig. 2). In this study, the Peak Ground Acceleration (PGA) values used for simulation calculations were derived from the equation proposed by Boulanger and Idriss in 2014, obtained from the Indonesian Seismic Source Map.

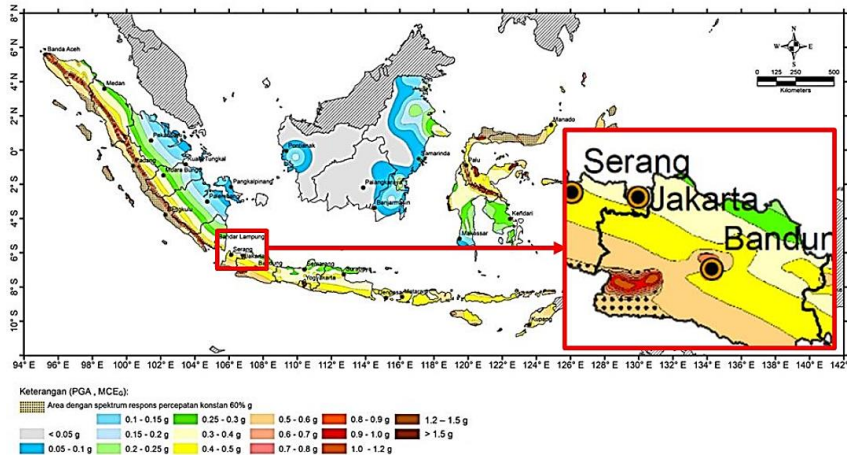


Figure 2. The PGA distribution map In Indonesia (modified from BSN 2019).

### 2.2 Geological Conditions in the Research Area

16 points from the reclamation island plan that were planned to be built in northern Jakarta were selected for interpreting the soil layer condition, and deemed to be representative of the entire research area. SPT tests were conducted on those 16 locations with depths of 20-30 meters below the ground surface. The illustration in Figure 3 delineates the distribution of SPT test points and the longitudinal and transverse section locations, providing a detailed depiction of the soil layer conditions pertinent to the reclamation island development plan.

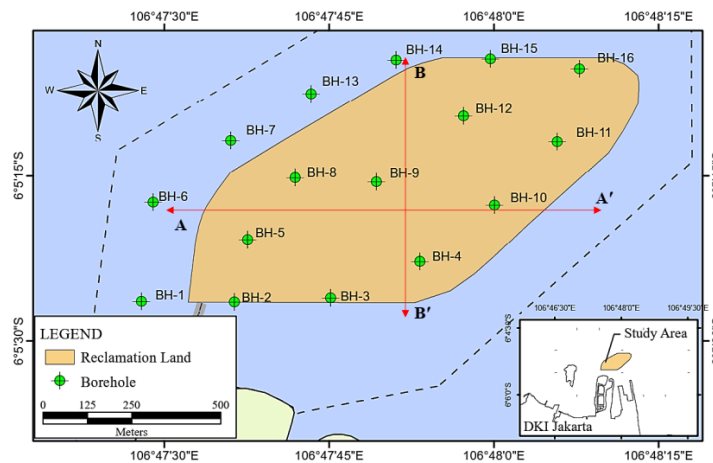


Figure 3. The layout of the reclamation island development plan and the distribution of field test data.

Figure 4 illustrates that the research area is predominantly composed of compact cohesive soil, with a maximum recorded N-SPT value of 50. Additionally, loose sand layers were observed at varying depths between 14 to 20 meters below the surface, exhibiting SPT values within the range of 20-30. The elevation of water at an average depth of 2.3 m above the ground surface results in the complete saturation of the entire soil. The presence of a thick cohesive soil layer makes it very difficult for water in the sand layer to drain out. In other words, this condition causes the water in the sand layer to be classified as undrained. Additionally, laboratory tests indicate that loose sand soil has amount of fine sand content, of around 5%. This value can subsequently be correlated with the category of soil type that is susceptible to liquefaction. According to Seed and Idriss (2001), sandy soil types that are prone to liquefaction have a fines content range of 5-35%.

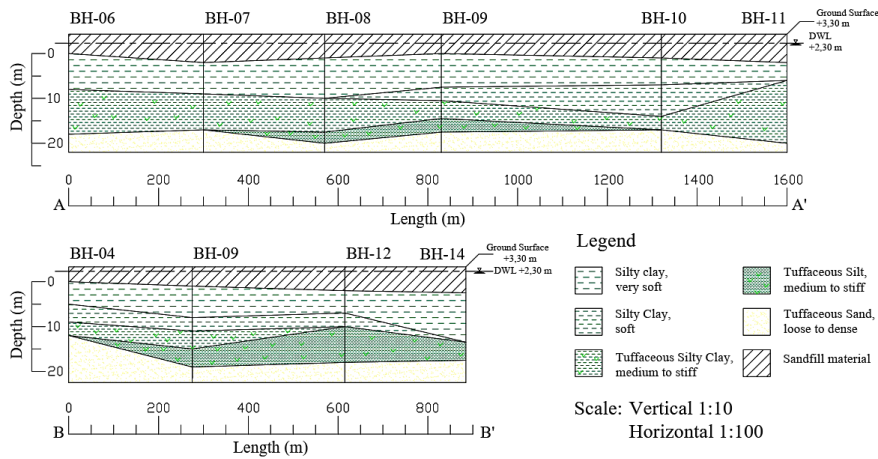


Figure 4. Interpretation of soil layer conditions.

### 2.3 Determination of Site Class

The classification of site classes within a given region serves the purpose of establishing seismic design criteria. The stages of calculations in classifying site classes according to SNI 1726-2019 (BSN, 2019), as shown in Equation (1) above, are consistent with the standard procedure. In the SNI, it is explained that soils with N-SPT values between 15 and 50, and less than 15, are classified as medium (SD) and soft (SE) soils, respectively. In this study, the water table is situated above the ground surface due to the reclamation island's location along the northern coast of Jakarta. The determination of the PGA value in the research area is assisted by using the 2017 Indonesian Seismic Source and Hazard Map.

$$\bar{N} = \frac{\sum_{i=1}^n d_i}{\sum_{i=1}^n \frac{d_i}{N_i}} \tag{1}$$

where  $\bar{N}$  represents the average standard field penetration resistance,  $N_i$  corresponds to the depth of each layer (i) in m, and  $d_i$  signifies the field penetration resistance at depth i. The liquefaction potential at a site is closely related to several factors such as peak ground acceleration and earthquake magnitude. The maximum earthquake peak acceleration is determined through a site-specific assessment, taking into consideration the site-specific amplification effects, as described in Equation (2) (BSN, 2019). Where  $a_{maks}$  represents the site-specific peak ground acceleration (m/s<sup>2</sup>) and  $F_{PGA}$  is the site coefficient.

$$a_{max} = F_{PGA} \cdot PGA \tag{2}$$

Based on the previous explanation, Figure 2 illustrates that Jakarta has a PGA range of 0.25-0.30 g. Several studies, such as Irsyam *et al.* (2014), interpret the PGA values for Jakarta using the PSHA method as ranging from 0.20 to 0.40 g. Meanwhile, according to the Indonesian Seismic Source Map, Jakarta specifically has a PGA value of 0.272 g. In this research, the PGA value utilized is 0.272 g. According to BSN (2019), soil can be categorized as soft soil through some parameters, such as mean shear velocity ( $\bar{V}_s$ ), mean SPT ( $\bar{N}$ ) and mean undrained shear strength ( $\bar{s}_u$ ). Furthermore, Table 3 shows the specific categories for determining site class conditions.

Table 3. Site class classification (BSN, 2019)

Site class	$\bar{V}_s$ (m/sec)	$\bar{N}$	$\bar{s}_u$ (kPa)
SD (medium soil)	175-350	15-50	50-100
	<175	<15	<50
SE (soft soil)	or any soil profile containing more than 3 meters with characteristics as follows:		
	1. plasticity index, PI > 20,		
	2. water content, w < 40e		
	3. undrained shear strength, su < 25 kPa		

### 2.4 Determination of Liquefaction Potential

Previous studies have investigated liquefaction potential using various methods. Wadi *et al.* (2021) identified the potential for liquefaction in the Benue region, Nigeria, using the Boulanger and Idriss method. The results of their study proved reliable with this method. This is substantiated by the simulation outcomes they conducted, demonstrating a correlation with the occurrences of liquefaction within the study region. Additionally, Farhangi *et al.* (2020) compared liquefaction potential calculation methods, including Boulanger and Idriss, Eurocode, and Juang. The findings showed that the Boulanger and Idriss method gave more closer results than another method. Based on these findings, this study adopts the Boulanger and Idriss (2014) calculation method. The fundamental principles of liquefaction evaluation were expounded by Boulanger and Idriss (2014) through the determination of the Cyclic Stress Ratio (CSR) and Cyclic Resistance Ratio (CRR). CSR is subsequently defined as a cyclic stress capable of inducing the liquefaction potential, while CRR represents a value denoting the cyclic resistance against the liquefaction potential. It has been asserted that laboratory test results reveal loose sandy soil with SPT values ranging from 22 to 30. Therefore, it is assumed the soil contains 5% of fines content. Thus rendering the CRR formula applicable. By using Seed and Idriss (1971) formula below,  $(N_1)_{60cs}$  could be obtained.

$$(N_1)_{60cs} = \alpha + \beta(N_1)_{60} \tag{3}$$

where  $\alpha$  dan  $\beta$  determined by the equation below.

$$\alpha = 0 \text{ for } FC \leq 5\% \tag{3.1}$$

$$\beta = 1 \text{ for } FC > 5\% \tag{3.2}$$

The value of CRR can be calculated using SPT criterion and the CSR is obtained through the following calculation.

$$CRR_{7,5} = \frac{1}{34 - (N_1)_{60cs}} + \frac{(N_1)_{60cs}}{135} + \frac{50}{[10(N_1)_{60cs} + 45]^2} - \frac{1}{200} \tag{4}$$

$$CSR_{7,5} = 0,65 \left( \frac{a_{max}}{g} \right) \left( \frac{\sigma_{vo}}{\sigma'_{vo}} \right) r_d \tag{5}$$

Where  $g$  is the gravitational acceleration ( $9,81 \text{ m/s}^2$ ),  $\sigma_{vo}$  dan  $\sigma'_{vo}$  are the total and effective overburden stresses ( $\text{kN/m}^2$ ), respectively, and  $r_d$  is the stress reduction coefficient at a specific depth. The safety factor (FS) against liquefaction is then determined using Equation (6). Liquefaction is considered not to occur if it has an FS value  $> 1$  and it is vulnerable to occur if it has an FS value lower or equal to 1 (Muley *et al.*, 2018).

$$FS = \left( \frac{CRR_{7,5} \times MSF}{CSR} \right) \tag{6}$$

The FS value obtained from semi-empirical method calculations is limited to initial predictions of liquefaction events. Hence, Iwasaki (1978) and Iwasaki *et al.*, (1982) developed a formula for determining the liquefaction potential index, which is more commonly known as LPI. The LPI value can be obtained using Equation (7). Where  $z$  is the depth of the midpoint of the soil layer (0 to 20 m) and  $dz$  is the incremental depth increment. The loading factor and the severity factor are defined as  $w(z)$  and  $F(z)$ , respectively.

$$LPI = \int_0^{20} F(z).w(z)dz \tag{7}$$

Although the framework and threshold LPI values proposed by Iwasaki *et al.* (1982) have demonstrated general utility, Maurer *et al.* (2014) revealed inaccuracies in predicting the occurrence or severity of liquefaction for a nontrivial percentage of sites. In their study, Maurer *et al.* (2014) provided an optimized LPI classification as indicated in Table 4. The LPI values obtained from each field test point will be mapped according to their potential occurrence categories. A microzoning map will be presented to provide a detailed and comprehensive representation of the distribution of liquefaction potential on the reclamation island along the northern coast of Jakarta.

Table 4. Potential liquefaction category based on LPI (Maurer *et al.*, 2014 after Iwasaki *et al.*, 1982).

LPI	Damage Classification
$LPI < 4$	No liquefaction
$4 \leq LPI < 8$	Marginal liquefaction
$8 \leq LPI < 15$	Moderate liquefaction
$LPI \geq 15$	Severe liquefaction
$LPI \geq 4$	Several Lateral Spreading

### 3 RESULTS AND DISCUSSION

#### 3.1 Seismic Design Analysis

By employing Equation (2), the peak ground acceleration at the surface can be presented as detailed in Table 5. It shows that twelve of sixteen test points are classified as soft soil and the last defined as medium soil. Most of the soft soil is spread over the whole reclamation land, while the medium soil is found at some point near the western and one point in the center of the research area. Table 3 in the previous section used to be the first step to determine the site class category.

Table 5. The classification of site classes in the research area.

No.	SPT		$a_{max} (g)$	No.	SPT		$a_{max} (g)$
	$\bar{N}$	Classification (BSN, 2019)			$\bar{N}$	Classification (BSN, 2019)	
BH-1	0.74	SE	0.46	BH-9	9.62	SE	0.46
BH-2	3.40	SE	0.46	BH-10	10.69	SE	0.46
BH-3	1.14	SE	0.46	BH-11	9.40	SE	0.46
BH-4	8.94	SE	0.46	BH-12	18.67	SD	0.36
BH-5	0.82	SE	0.46	BH-13	1.60	SE	0.46
BH-6	16.83	SD	0.36	BH-14	8.94	SE	0.46
BH-7	15.36	SD	0.36	BH-15	1.45	SE	0.46
BH-8	18.33	SD	0.36	BH-16	1.19	SE	0.46

#### 3.2 Evaluation of Liquefaction Potential

Liquefaction potential analysis was performed at each field test point. Table 6 illustrates an example of the calculation of the liquefaction safety factor at BH-4. Figure 5 presents a comparison of values between  $(N1)_{60cs}$ , CSR, and CRR, along with their impact on FS at 2-meter depth intervals. The graph reveals a correlation between FS values and measurement depth. It appears that there is a tendency for an increase in the values of both  $(N1)_{60cs}$ , FS, CSR, and CRR. This indicates that the soil in the research area represented by the specified point will significantly become safer. This is attributed to the increased overburden pressure on the soil itself. The rest of SPT test indicates the typical result of liquefiable and non-liquefiable soil at a certain depth.

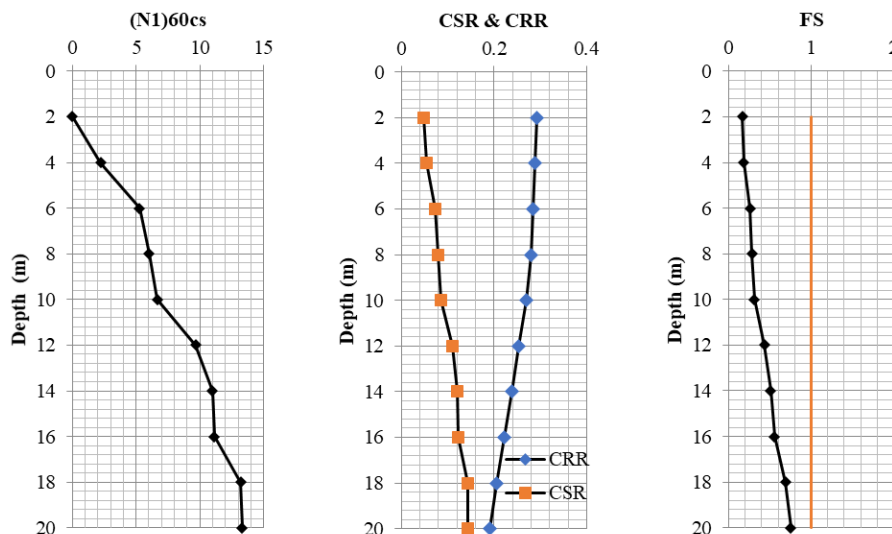


Figure 5. Site corresponding data results for BH-4.

Table 6. The summary value of FS in BH-4.

No.	Depth (m)	(N <sub>1</sub> ) <sub>60cs</sub>	γ (kN/m <sup>3</sup> )	CSR	CRR	FS	Classification
1	2.00	0.00	13.20	0.29	0.05	-	silty clay, very soft
2	4.00	2.20	13.20	0.29	0.06	-	
3	6.00	5.26	15.20	0.28	0.08	-	
4	8.00	6.00	15.20	0.28	0.08	-	silty clay, soft
5	10.00	6.66	15.30	0.27	0.09	-	tuffaceous silty clay, medium stiff to stiff
6	12.00	9.68	15.30	0.25	0.12	-	
7	14.00	10.98	18.70	0.24	0.13	0.54	Liquefiable
8	16.00	11.14	18.70	0.22	0.13	0.58	Liquefiable
9	18.00	13.22	18.70	0.21	0.15	0.73	Liquefiable
10	20.00	13.33	18.70	0.19	0.15	0.79	Liquefiable

Table 7 provides a summary of potential liquefaction events at that specific point. Based on the liquefaction potential calculations, it is apparent that several areas have a significant degree of low vulnerability. Figure 6, generated using QGIS software by using linear distance weighting interpolation methods, illustrates the spatial distribution of liquefaction potential categorized into four vulnerability levels: no liquefaction, marginal liquefaction, and moderate liquefaction. While the predominant potential falls within the no liquefaction category, as observed at points BH-1, BH-2, BH-5, and so forth, it should be noted that areas within the research site also exhibit a marginal and moderate potential for liquefaction events. This phenomenon arises due to variations in the thickness of the sand layers at each test point. Certain test points indicate that as the thickness of a sand layer increases or decreases, the corresponding evaluation of safety factors tends to be lower, rendering them susceptible to liquefaction. This is particularly evident in the southeastern region of the reclamation island, including points BH-4, BH-8, BH-9, and BH-10. Consequently, it is imperative to consider proactive measures to mitigate potential incidents and future losses.

Table 7. LPI and SF min value on each borehole

No.	Σ LPI	Classification	FS min	No.	Σ LPI	Classification	FS min
BH-1	0.93	No liquefaction	0.77	BH-9	5.39	Marginal liquefaction	0.74
BH-2	0.74	No liquefaction	0.81	BH-10	5.14	Marginal liquefaction	0.55
BH-3	0.00	No liquefaction	0.17	BH-11	0.00	No liquefaction	0.54
BH-4	9.86	Severe liquefaction	0.43	BH-12	0.75	No liquefaction	0.81
BH-5	0.74	No liquefaction	0.82	BH-13	0.78	No liquefaction	0.80
BH-6	0.00	No liquefaction	0.93	BH-14	4.77	Marginal liquefaction	0.57
BH-7	1.58	No liquefaction	0.91	BH-15	0.81	No liquefaction	0.80
BH-8	5.71	Marginal liquefaction	0.98	BH-16	0.00	Non-liquefiable	-

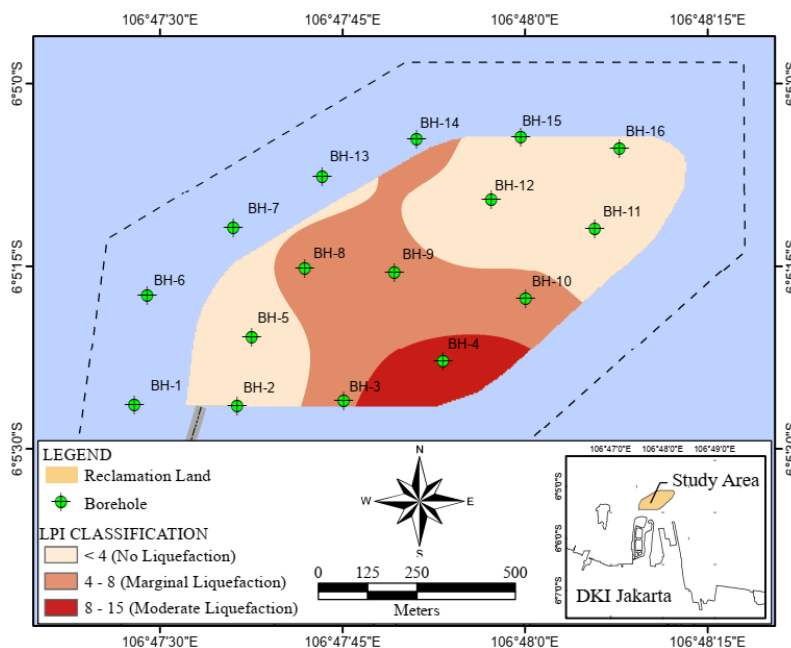


Figure 6. Microzonation map of liquefaction susceptibility in reclamation land (based on linear distance weighting interpolation methods).

#### 4 CONCLUSION

Soil layer composition under the reclamation island on the northern coast of Jakarta is characterized by a predominant presence of cohesive soils, encompassing soft, medium, and stiff clays. Layers of loose sand can be encountered at a minimum depth of 14 meters below the surface. The sandy conditions, which tend to be saturated, loose, and lacking drainage, significantly increase the liquefaction potential or, at the very least, sand boiling during a seismic event of sufficient intensity and duration.

The map results of analytical calculations regarding liquefaction potential using the simplified procedure method and linear distance weighting interpolation method indicate that the potential for liquefaction events in the research area tends to be predominantly categorized as no potential (53,26% of the island area). Nevertheless, areas with a marginal to moderate potential for liquefaction, such as BH-4, BH-8, BH-9, and BH-10 cover 46,74% of the island area. Thus still needs to be considered to prevent the occurrence of liquefaction events in the future.

#### ACKNOWLEDGMENTS

The author would like to express their gratitude for the support given by The Indonesian Ministry of Public Works and Public Housing, PT. Taman Harapan Indah and Center of Excellence of Technological Innovation for Disaster Mitigation (GAMA-InaTEK) Universitas Gadjah Mada for providing relevant data and valuable information for this study.

#### REFERENCES

- Agung, P. A., Sultan, R., Idris, M., Sudjianto, A. T., Ahmad, M. A., & Hasan, M. F. (2023). "Probabilistic of in Situ Seismic Soil Liquefaction Potential Based on CPT-Data in Central Jakarta, Indonesia". *International Journal of Sustainable Construction Engineering and Technology*, 14(1), 241-248.
- Bock, Y., Prawirodirdjo, L., Genrich, F., Stevens, C. W., McCaffrey, R., Subarya, C., . . . Calais, E. (2003). "Crustal motion in Indonesia from Global Positioning System measurements". *Journal of Geophysical Research: Solid Earth*, 108(B8).
- Boulanger, R. W., & Idriss, I. M. (2014). "CPT and SPT based liquefaction triggering procedures". *Report No. UCD/UGM. -14, 1*. Center for Geotechnical Modeling.
- BSN. (2019). *SNI 1726-2019*. Badan Standardisasi Nasional.
- Dinata, I. A., Darlan, Y., Sadisun, I. A., Pindratno, H., & Saryanto, A. (2018). "Liquefaction hazard analysis for infrastructure development in Gulf of Jakarta". *AIP Conference Proceedings* (pp. Vol. 1730, No.1). Bandung: AIP Publishing.
- Farhangi, V., Karakouzian, M., & Geertsema, M. (2020). "Effect of micropiles on clean sand liquefaction risk based on CPT and SPT". *Applied Sciences*, 10(9), 3111.
- Hamilton, W. B. (1979). "Tectonics of the Indonesian region". Vol. 1078. US Government Printing Office.
- Irsyam, M., Hutabarat, D., Asrurifak, M., Imran, I., Widiyantoro, S., Hendriyawan, . . . Pandhu, R. (2015). "Development of Seismic Risk Microzonation Maps of Jakarta City". *Geotechnics for catastrophic flooding events*, 35-47.
- Iwasaki, T. (1978). "A practical method for assessing soil liquefaction potential based on case studies at various sites in Japan". *Proceeding of 2nd International Conference on Microzonation*, (pp. 885-896). San Fransisco.
- Iwasaki, T., Tokida, K. I., Tatsuoka, F., Watanabe, S., Yasuda, S., & Sato, H. (1982). "Microzonation for soil liquefaction potential using simplified methods". *Proceedings of the 3rd international conference on microzonation*, (pp. 1310-1330). Seattle.
- Jalil, A., Fathani, T. F., Satyarno, I., & Wilopo, W. (2020). "A study on the liquefaction potential in banda aceh city after the 2004 sumatera earthquake". *GEOMATE Journal*, 147-155, 18(65).
- Mase, L. Z. (2018). "One-dimensional site response analysis of liquefaction potential along coastal area of Bengkulu City, Indonesia". *Civil Engineering Dimension*, 20(8), 57-69.
- Mase, L. Z., Likitlersuang, S., Tobita, T., Chaiprakaikew, S., & Soralump, S. (2020). "Local site investigation of liquefied soils caused by earthquake in Northern Thailand". *Journal of Earthquake Engineering*, 24(7), 1181-1204.
- Maurer, B. W., Green, R. A., Cubrinovski, M., & Bradley, B. A. (2014). "Evaluation of the liquefaction potential index for assessing liquefaction hazard in Christchurch, New Zealand". *Journal of Geotechnical and Geoenvironmental Engineering*, 140 (7), 040140332.
- Muley, P., Maheshwari, B. K., & Paul, D. K. (2018). "Assessment of liquefaction potential index for Roorkee region". *16th Symposium on earthquake engineering*.

- Seed, H. B., & Idriss, I. M. (1971). "Simplified procedure for evaluating soil liquefaction potential". *Journal of the Soil Mechanics and Foundation division*, 97(9), 1249-1273.
- Wadi, D., Wu, W., Malik, I., Ahmed, H. A., & Makki, A. (2021). "Assessment of liquefaction potential of soil based on standard penetration test for the upper Benue region in Nigeria". *Environmental Earth Sciences*, 80, 1-11.